Strain softening is not present during axial extensions of rat intact right ventricular trabeculae in the presence or absence of 2,3-butanedione monoxime

R. S. Kirton, A. J. Taberner, A. A. Young, P. M. F. Nielsen and D. S. Loiselle

Am J Physiol Heart Circ Physiol 286:708-715, 2004. First published Oct 9, 2003;
doi:10.1152/ajpheart.00580.2003

AJP - Heart and Circulatory Physiology publishes original investigations on the physiology of the heart, blood vessels, and lymphatics, including experimental and theoretical studies of cardiovascular function at all levels of organization ranging from the intact animal to the cellular, subcellular, and molecular levels. It is published 12 times a year (monthly) by the American Physiological Society, 9650 Rockville Pike, Bethesda MD 20814-3991. ISSN: 0363-6135, ESSN: 1522-1539. Visit our website at http://www.the-aps.org/.

Am J Physiol Heart Circ Physiol 286: H708–H715, 2004;
10.1152/ajpheart.00580.2003.

Strain softening is not present during axial extensions of rat intact right ventricular trabeculae in the presence or absence of 2,3-butanedione monoxime

R. S. Kirton,[1,3] A. J. Taberner,[1,5] A. A. Young,[1,2,4] P. M. F. Nielsen,[1,3] and D. S. Loiselle[1,4]

[1]*Bioengineering Institute and Departments of* [2]*Anatomy,* [3]*Engineering Science, and* [4]*Physiology, The University of Auckland, Auckland 1001, New Zealand; and* [5]*Department of Mechanical Engineering, Massachusetts Institute of Technology, Cambridge, Massachusetts 02139-4307*

Submitted 23 June 2003; accepted in final form 2 October 2003

Kirton, R. S., A. J. Taberner, A. A. Young, P. M. F. Nielsen, and D. S. Loiselle. Strain softening is not present during axial extensions of rat intact right ventricular trabeculae in the presence or absence of 2,3-butanedione monoxime. *Am J Physiol Heart Circ Physiol* 286: H708–H715, 2004; 10.1152/ajpheart.00580.2003.—Recent studies of passive myocardial mechanics have shown that strain softening behavior is present during both inflation of isolated whole rat hearts and shearing of tissue blocks taken from the left ventricular free wall in pigs. Strain softening is typically manifested by a stiffer force-extension relation in the first deformation cycle relative to subsequent cycles and is distinguished from viscoelasticity by a lack of recovery of stiffness, even after several hours of rest. The causes of this behaviour are unknown. We investigated whether strain softening is observed in uniaxial extensions of intact, viable, rat right ventricular (RV) cardiac trabeculae. Stretch and release cycles of 5%, 10%, and 15% muscle length were applied at a constant velocity at 26°C. Muscles were tested in random order in the presence and absence of 50 mM 2,3-butanedione monoxime (BDM). Whereas strain softening was displayed by nonviable trabeculae, it was not observed in viable preparations undergoing physiologically relevant extensions whether in the presence or absence of BDM. BDM also had no effect on passive compliance. There was a reversible increase of muscle compliance between the first and subsequent cycles, with recovery after 30 s of rest, independent of the presence of BDM. We conclude that strain softening is neither intrinsic to viable rat RV trabeculae nor influenced by BDM and that passive trabeculae compliance is not altered by the addition of BDM.

cardiac muscle; passive tissue compliance; stress-strain relations; stretch

THE PASSIVE MECHANICAL PROPERTIES of cardiac muscle are of fundamental importance, as they influence the velocity of shortening (8), limit the volume of blood that enters the heart, and play a major role in determining the stroke volume (5). It is crucial for our understanding of the mechanisms by which cardiovascular disease changes the mechanical properties of the diseased heart to have a sound understanding of the passive material properties of healthy cardiac tissue. Impaired diastolic filling can also manifest as diastolic heart failure in patients with apparently normal systolic function.

However, the passive tension-length relationship is difficult to determine at the tissue level due to the complex three-dimensional geometry of the heart and the laminar microstructure of myocardium (6, 26, 35, 44). To reduce the anatomic and microstructural complexities present in a whole heart model, mechanical experiments are often conducted on smaller samples of myocardial tissue. Such experiments range from biaxial testing of myocardial sheets (10) to uniaxial testing of ventricular strips (33), papillary muscles (4, 16), cardiac trabeculae (42), isolated myocytes (5, 17), myofibrils (29), actin filaments (30), and individual titin molecules (25). Anisotropic, nonlinear, large-deformation material behavior has been observed together with strain history-dependent and strain rate-dependent phenomena.

It is well known that myocardium exhibits viscoelastic behavior because the stress response depends on strain history and strain rate. However, strain softening phenomena have also been observed in which the myocardial stress-strain relation depends on the maximum strain state obtained in an experimental protocol. This is typically manifested as a stiffer stress-strain relationship on the first loading cycle than in all subsequent cycles. On stretching to a new maximum strain level, the stress-strain relation follows the previously recorded curve up to the previous maximum strain level. Subsequent repetitions to the new maximum level follow a new, softer stress-strain relationship. Figure 1 illustrates a typical strain softening response. Unlike viscoelastic behavior, the tissue does not recover, even after several hours of rest.

Emery et al. (13, 14) measured the pressure-volume relation and strain softening behavior of whole rat hearts and found that the "preconditioning" behavior observed was better explained by a strain softening model than by viscoelastic effects. Dokos et al. (12) subjected blocks of pig ventricular myocardium to simple shear deformations and recorded strain softening behavior even at low levels of strain. Both these studies reported strain softening well within the physiological range. Linke et al. (27) found strain softening in isolated rabbit cardiac myofibrils but only at sarcomere length (SL) extensions above 2.7 μm, which is greater than the normal physiological SL extension. Because all of the collagen had been removed, this strain softening was attributed to titin being nonreversibly altered. In contrast to this result, Kellermayer et al. (25) measured reversible softening in single titin molecules, which was described as "mechanical fatigue." This softening occurred at low levels of stress, comparable with those reached by skeletal muscle when stretched to 2–3 μm SL.

Possible causes of myocardial strain softening include damage to elastic constitutive components (13, 14), fluid shifts, or rearrangement of microstructural components. However, studies that used the chemical phosphatase 2,3-butanedione monoxime (BDM) may also have been influenced by the effect of

Address for reprint requests and other correspondence: R. S. Kirton, Bioengineering Institute, The Univ. of Auckland, 70 Symonds St., Auckland 1001, New Zealand (E-mail: r.kirton@auckland.ac.nz).

The costs of publication of this article were defrayed in part by the payment of page charges. The article must therefore be hereby marked "*advertisement*" in accordance with 18 U.S.C. Section 1734 solely to indicate this fact.

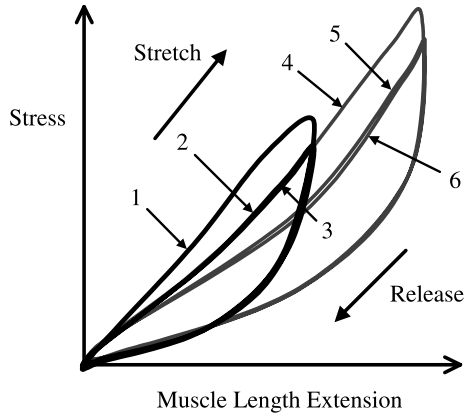

Fig. 1. Schematic depiction of irreversible strain softening. The steepest curve (*curve 1*) represents stress-muscle length (ML) extension for the first level of stretch, with subsequent cycles to this level (*curves 2* and *3*) having softened to a lower stiffness. *Curves 4–6* represent a new level of maximum stretch. The first extension to the new level (*curve 4*) follows the same curve as the softened curves (*curves 2* and *3*) from the previous level. The subsequent cycles (*curves 5* and *6*) once again follow a softened stress-ML extension curve.

this drug on cross-bridge action and mechanical stiffness. The negative inotropic action of BDM on cardiac tissue was first demonstrated by Wiggins et al. (43) in 1980. BDM has been shown to protect human cardiac tissue from cutting injury (34), delay the onset of rigor in isolated chick and rabbit myocytes (22), and delay the onset of rigor as well as the depletion of ATP and creatine phosphate in ferret papillary muscle (19). Although BDM has been unanimously reported to inhibit contractile force in a dose-dependent manner, its effects on calcium transients, intracellular calcium concentration, and action potentials are less well defined (for a review, see Ref. 38). It appears to affect multiple sites in the excitation-contraction coupling pathway, with each site having a different and dose-dependent response. The effects of BDM also appear to be temperature, Ca^{2+} concentration, and species dependent. The effects of BDM on passive tissue properties have not been fully explored, although BDM has been reported to affect the passive pressure-volume relationship of in vivo porcine hearts (31). Because BDM is presumed to increase the proportion of cross-bridges in the weakly bound state in activated cardiac tissue (45), the presence of BDM in quiescent cardiac tissue may induce a similar increase in the proportion of weakly bound cross bridges and hence increase the observed strain softening.

The objective of the present study was to ascertain whether strain softening occurs in intact healthy rat cardiac trabeculae and, if so, whether high concentrations of BDM, as used in studies of Dokos et al. (12) (50 mM) and Emery et al. (13, 14) (30 mM), is an exacerbating factor. The use of isolated trabeculae, as opposed to whole hearts or blocks of ventricular tissue, allowed improved measurement of muscle length extension while minimizing damage due to specimen preparation and allowing an adequate diffusive supply of oxygen. The trabecula preparation is a thin, naturally occurring collection of axially aligned myocytes. Mounted between a force transducer and an actuator, it has been extensively used for the examination of myocardial mechanical properties since the seminal paper by ter Keurs et al. (42). We used these preparations from the rat right ventricle to answer the following questions: *1*) Is strain softening behavior exhibited in viable intact cardiac trabeculae [cf. intact hearts (13, 14) and ventricular myocardial blocks (12)]? *2*) Is strain softening influenced by the presence of BDM? and *3*) Does BDM affect the passive force-length relationship of cardiac trabeculae?

MATERIALS AND METHODS

Muscle Preparation and Solutions

All experiments were approved by the University of Auckland Animal Ethics Committee. Wistar rats (age 71 ± 28 days, weight 303 ± 38 g, means ± SD) were stunned and immediately decapitated. The heart was quickly excised and plunged into dissection solution at 0°C to induce arrest. After the aorta was cannulated, the coronary vasculature was perfused using the Langendorff technique.

The criteria for selection of right ventricular trabeculae were similar to those described by de Tombe and ter Keurs (9). Unbranched, geometrically uniform specimens were sought that ran freely from the right ventricular free wall to the atrioventricular ring and were relatively long (2.52 ± 0.87 mm, $n = 10$) and sufficiently thin (207 ± 41 μm) to ensure adequate oxygenation (37). The trabecula preparation, including blocks (~300 × 300 × 600 μm) of tissue at each end for mounting, was excised from the ventricular wall. When the preparation was transferred to the muscle bath, the transferral method avoided pulling the trabeculae through fluid menisci.

The superfusate was a modified Tyrode solution [containing (in mM) 141.6 NaCl, 5.97 KCl, 1 $MgCl_2$, 1.18 NaH_2PO_4, 10 HEPES, 10 glucose, and 0.5 $CaCl_2$]. The pH was adjusted to 7.4 by the addition of 1 M Tris. To form the dissection solution, the Tyrode solution was supplemented with 20 mM BDM. During experiments, preparations were superfused with the Tyrode solution in either the presence (+BDM, 50 mM) or absence (−BDM) of BDM. A concentration of 50 mM BDM was chosen to emulate the Dokos et al. study (12), in which strain softening was measured. Solutions were vigorously bubbled with 100% O_2. All chemicals were purchased from Sigma Aldrich and were of analytic grade. All experiments were conducted at 26°C.

Muscle Bath and Superfusate Delivery System

The U-shaped muscle bath (2 × 2 × 10 mm, volume 40 μl) was mounted on a Peltier device (MI 1023 TAC, 9.2 W, Marlow Industries), which was, in turn, mounted on an X-Y-Z micromanipulator (MicroMech, Coherent). This system had a working temperature range of 10–50 ± 0.1°C. Surface tension constrained the superfusate within the open-topped and open-ended bath, while the superfusate flow was controlled by two peristaltic pumps (Minipuls III, Gilson). To allow electric field stimulation of the trabecula, two 100-μm-diameter platinum wire electrodes were situated either side of the muscle bath. An SD9 Stimulator (Grass Instruments) provided the stimulus.

Data Acquisition and Experimental Control

A Pentium 3-equivalent personal computer was used for data acquisition and experimental control. Data acquisition, motor control, and image processing were achieved using software custom written in LabView 5.1 (National Instruments), a data-acquisition card (PCI 6031E, National Instruments), a four-axis motor controller card (PCI 7344, National Instruments), and a digital frame-grabber card (PCI FG-3170 CameraLink, Silicon Imaging).

Muscle Attachment

An end-on muscle attachment system was constructed using glass hooks fashioned from thin glass tubing (500 μm inner diameter with a wall thickness of 50 μm, VitroCom). One hook was attached to the strain gauge, and the second hook was attached to the mechanical

perturbation system. The trabecula was carefully maneuvered into the hooks, which were then separated until the trabecula was gently held. Care was taken not to stretch the muscle beyond resting length.

Force Measurement

Force was measured via a silicon beam strain gauge (model AE-801, SensoNor), which was attached to a well-damped, three-axis micromanipulator (Prior Scientific; Cambridge, UK), and amplified by a factor of 400. This system had a sensitivity of 1.262 V/N with 10 μN resolution.

Mechanical Perturbation System

Mechanical perturbation was supplied via a high-resolution linear actuator (M-227.25 DC-Mike, Physik Instrumente), which was controlled via the four-axis motor controller card. The first resonant frequency of the complete mechanical system was above 1 kHz.

Optical Systems

A Wild8 stereomicroscope (Leica), a color charge-coupled device camera (1CD-800P, Ikegami), and a monitor (PVM-1454QM Trinitron, Sony) aided in the manipulation, mounting, and monitoring of trabeculae during the course of the experiment.

A second microscope system obtained high-magnification images of sections of the trabecula, from which an estimation of SL was calculated. This microscope system was composed of the following components: a ×50 objective lens (No. 101950, LWD MSP Plan, Olympus), an Infinitube in-line assembly (No. L54-590, Edmund Optics), a video camera (SI-3170 MegaCamera, Silicon Imaging), a frame grabber (FG-3170 CameraLink card, Silicon Imaging), and a controlling computer. The camera, in conjunction with the ×50 objective lens and Infinitube, gave a 120 × 90 μm field of view. An automated X-Y-Z micromanipulator stage (M425 series, Newport) and the four-axis motor controller card were used to position the SL microscope objective lens.

A fast Fourier transform technique, similar to that validated by Dobesh et al. (11), was used to calculate the average SL within the field of view. The system was calibrated with 600 and 200 lines/mm diffraction gratings and gave a measured accuracy of ~6 nm. This system was used to set the resting SL to ~1.9 μm and to calculate the SL extension during experimental protocols.

Mounting of the Muscle

After the trabecula was mounted in the muscle bath, the resting SL was measured. If the SL was <1.9 μm, the muscle length (ML) was increased until SL reached 1.9 μm. If the SL was >1.9 μm, then ML was not reduced (to avoid preconditioning the muscle). The average resting SL was 1.97 ± 0.06 μm, whereas the longest SL induced during the 15% ML stretches was 2.28 μm.

If undue spontaneous activity was present when the specimen was at its operating temperature of 26°C, the muscle was excluded from analysis (9). Each trabecula was stimulated (rectangular, 4-ms duration, 0.2 Hz, 20% supramaximal voltage) until its force response stabilized (minimum of 10 min). After stabilization, the resting SL was remeasured; if the preparation had shortened due to the elicited twitches, then it was lengthened back to the prestimulation SL.

Experimental Protocols

The goals of this study were to ascertain the existence of strain softening in intact rat trabeculae in the presence and absence of 50 mM BDM. The mechanical perturbation protocol used to measure strain softening was similar to that used by Dokos et al. (12) on blocks of ventricular tissue. Each trabecula was subjected to six ML extension-and-release cycles (Cycles), where the extensions were 5%, 10%, and 15% ML (Stretch). After a 10-min rest interval, the 15% ML Stretch was repeated to test for recovery of stress. This series of six Cycles at three Stretches, plus repetition of the 15% Stretch, is referred to as one Set. Stretches were conducted at a constant velocity of 25 μm/s. Upon completion of a Set, the viability of the trabecula was assessed via twitch force. Provided that active muscle performance remained satisfactory, up to four Sets were then performed. Strain softening was assessed by comparing the stresses at a given ML extension: *1*) between Stretches within *Set 1*, and *2*) between corresponding Cycles (*Cycles 1–6*) of *Set 1* and *Set 2*.

The effect of BDM on strain softening was examined by subjecting five trabeculae to +BDM in *Set 1* and to −BDM in *Set 2*. Another five trabeculae were tested in the converse order. This allowed the effect of BDM to be determined independent of the order in which the tests were performed (denoted as Order below).

Stress was defined as force per (ellipsoidal) cross-sectional area (estimated from top and side dimensions). For the trabeculae used in this study, the peak twitch force measured at resting SL (1.97 ± 0.06 μm) was 25.9 ± 7.4 kPa (26°C, 0.5 mM Ca^{2+}). Note that to avoid preconditioning, SL was not increased to give maximal twitch force.

Statistical Analysis

Data were subjected to repeated-measures ANOVA as appropriate for a 3 × 4 × 6 (Set × Stretch × Cycle) design. Differences among levels of statistically significant ($P < 0.05$) main effects or interactions were sought, post hoc, using appropriate sets of mutually orthogonal contrast coefficients. All analyses were performed using SAS software. Unless otherwise stated, all data are presented as means ± SE.

RESULTS

Testing for Strain Softening in Quiescent Viable Trabeculae

A typical example of the stresses induced upon subjecting a quiescent trabecula to its first Set of length perturbations, consisting of 5%, 10%, and 15% Stretches, is plotted in Fig. 2. Note the absence of irreversible strain softening. Similarly, strain softening is not apparent in Fig. 3, which compares the 15% Stretches between *Set 1* (−BDM) and *Set 2* (+BDM).

In Figs. 2 and 3, the observed hysteresis loops demonstrate energy dissipation consistent with the presence of viscoelastic material properties. A small degree of softening was observed

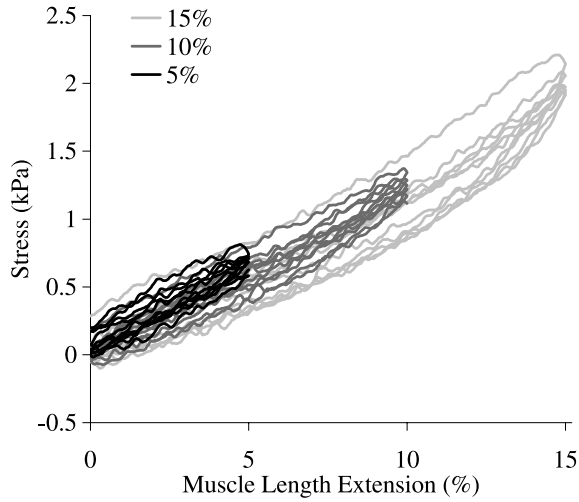

Fig. 2. Typical stress-ML extension data measured in *Set 1* [without 2,3-butanedione monoxime (−BDM)]. The trabecula was subjected to 6 cycles of 5% (solid line), 10% (dark gray line), and 15% (light gray line) ML extension at 25 μm/s. Irreversible strain softening was not observed, as the first extension curves for all three Stretches followed the same stress-ML extension curve.

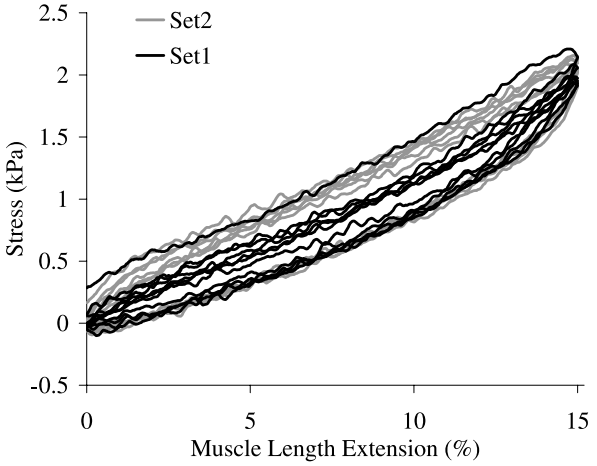

Fig. 3. Stress-ML extension curves showing 6 cycles of 15% ML extension measured during *Set 1* (−BDM, solid line) and *Set 2* (+BDM, light gray line). For these data, the first stress-ML extension curves for *Set 1* and *Set 2* overlay, thus failing to show irreversible softening.

between the first and subsequent Cycles of each Stretch (Figs. 2 and 3), which recovered before the next Stretch. This reversible softening can be understood in terms of viscoelasticity but not in terms of irreversible strain softening.

Figure 4*A* presents stress as a function of SL, illustrating that viscoelastic softening also occurs at the SL level. Figure 4*B* shows that SL faithfully tracks ML across the full range of extensions. The nearly linear form of the relationship indicates that end compliance is roughly proportional to midtrabecula compliance for these low extensions. Because SL data were acquired only 12 times per cycle, and no stress-SL plots showed any signs of strain softening (Fig. 4*A*), subsequent statistical analyses were undertaken using ML data, which were sampled more frequently. Note that across all the experiments used in this study, SLs between 1.9 and 2.28 μm were observed during the 15% ML extensions of viable trabeculae.

In the presence of strain softening, any given ML extension would induce a maximum stress the first time the muscle experiences that level of extension. Therefore, the first 5% ML cycle would have the steepest stress-strain relationship, with the following five cycles (at 5% ML extension) showing a more compliant stress-strain relationship. The same softening process would also be observed when the ML stretch was increased to 10% and again to 15%. Thereafter, strain softening would not be observed if the ML extensions were less than or equal to 15%.

Several methods were applied to detect strain softening in the stress-ML extension data. Initially, the stresses measured at 3.5% ML extension were compared across all six Cycles within all four Stretches of *Set 1* and *Set 2* using repeated-measures ANOVA. For Stretches of 10% and 15%, a similar analysis was conducted using the stresses measured at 7% ML extension. The ANOVA examined the statistical significance of the five main effects (Order, BDM, Cycle, Stretch, and Set) and all possible interactions on stress. The ANOVA results are summarized in Table 1. Figure 5 summarizes the Cycle × Set interactions for both the 3.5% and 7% ML extensions. Note that, for each extension, the statistical power to detect a significant difference (had one existed) was considerable, because the *F* ratio arising from the repeated-measures ANOVA has 5 and 35 degrees of freedom for the numerator and denominator, respectively. Muscle stiffness did not decrease between *Set 1* and *Set 2* for either extension, thereby indicating an absence of strain softening. Likewise, BDM had no effect at either extension. Furthermore, there was neither an Order main effect nor a BDM × Order interaction. These results preclude an effect of BDM on passive stress in any of our protocols. Not surprisingly, there was a significant effect of Cycle on stress ($P < 0.0001$), due to reversible viscoelastic softening. The interaction of Stretch and Cycle was also significant, indicating that Stretch size had an effect on the extent of reversible softening. No other interactions were statistically significant. Post hoc analysis revealed that for both ML extensions, stress was significantly larger during the first cycle, with no significant differences among *Cycles 2–6*. The value of stress in *Cycle 1* (averaged across all Stretches) did not differ between *Set 1* and *Set 2* (Fig. 5). Thus no test showed the presence of strain softening.

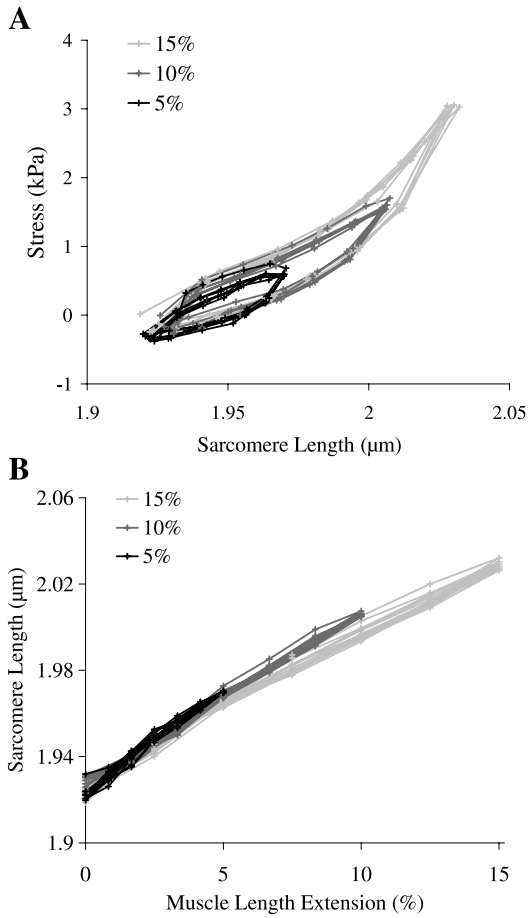

Fig. 4. Stress-length relations. *A*: stress-sarcomere length (SL) relation measured when a quiescent trabecula was subjected to 6 cycles of 5% (solid line), 10% (dark gray line), and 15% (light gray line) ML extension. +, SL measurements from acquired images (joined via linear interpolation). No evidence of strain softening was observed, as stress-SL data follow same curve. *B*: SL versus ML extension from a quiescent trabecula (same as in *A*) subjected to 6 cycles of 5% (solid line), 10% (dark gray line), and 15% (light gray line) ML extension. The relationship is approximately linear and repeatable over this range of SL extensions. Note that the data presented here are from the trabecula that demonstrated the highest degree of end compliance of those trabeculae included in the study. The average SL extension for the trabeculae used in this study, as measured during the 15% ML extensions, was 9.4%.

Table 1. *ANOVA-derived P values of main effects and selected interactions on stress at 3.5% and 7% ML for Set 1 and Set 2*

	ML Extension	
	3.5%	7%
Set 1 versus *Set 2*	0.8050	0.6515
Order BDM presented	0.5775	0.7312
+BDM versus −BDM	0.6841	0.9225
Magnitude of Stretch (5%, 10%, and 15%)	0.1350	0.4702
Cycle (*1–6*)	0.0001	0.0001
Order × BDM	0.7827	0.6923
Order × Set	0.6985	0.8126
Set × Stretch	0.4326	0.2983
Set × Cycle	0.4658	0.2426
Stretch × Cycle	0.0095	0.0348

Values shown are ANOVA-derived probabilities (*P* values) arising from tests of significance of main effects and selected interactions on stress at 3.5% and 7% muscle length (*Set 1* and *Set 2*); $n = 10$ preparations. Note the lack of significant difference between *Set 1* and *Set 2* (no strain softening) and the lack of effect of the order in which tests were performed (Order) × 2,3-butanedione monoxime (BDM) (no effect of BDM on strain softening. Stretch, extensions at 5%, 10%, and 15% ML; Cycle, extension-and-release cycle.

Despite these null results, we devised and tested two additional indexes of strain softening. The first involved calculating the average stress difference between *Cycle 1* and *Cycle 6*, *Cycle 2* and *Cycle 6*, etc., for each value of Stretch. The second was to find the average stress difference between *Cycle 1* of *Set 1* and *Cycle 1* of *Set 2* for each of the 5%, 10%, and 15% ML Stretches. In both cases, the average difference values were then subjected to ANOVA, as above. In neither case (data not presented) did we obtain any evidence of strain softening in either the presence or absence of BDM.

In contrast to the lack of strain softening found in viable trabeculae, Fig. 6 shows evidence of strain softening behavior during one Set of stretches (5%, 10%, and 15%) of a trabecula that had become electrically nonresponsive. Such behavior was found in all trabeculae that ceased to respond to electrical stimulation.

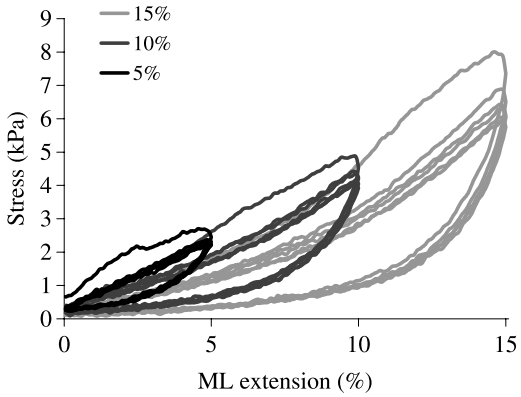

Fig. 6. Stress-muscle length extension data recorded from a trabecula that no longer responded to electrical stimulation. Strain softening is apparent. (Note the difference of stress scale vis-à-vis Figs. 2–5 and 7.)

Effect of BDM on the Compliance of Quiescent Trabeculae

To determine the effect of BDM on the diastolic compliance of passive cardiac trabeculae, the stresses measured at 3.5% and 7% ML extension were compared between *Set 2* and *Set 3*, where the presence or absence of BDM was reversed between Sets ($n = 9$). Comparison of *Set 2* and *Set 3* removed any potential strain softening artifacts, because the maximum strain level of 15% had already been reached in *Set 1*.

With the use of the same techniques as those for the first index of strain softening (above), the stresses at 3.5% and 7% ML extension for both *Set 2* and *Set 3* were compared across Stretches (Fig. 7). ANOVA revealed no significant effect of BDM for either the 3.5% ($P > 0.43$) or 7% ($P > 0.28$) ML extensions (Table 2).

DISCUSSION

Strain Softening

To our knowledge, this is the first study that has attempted to measure irreversible strain softening in viable intact cardiac trabeculae of any species. The term strain softening is applied

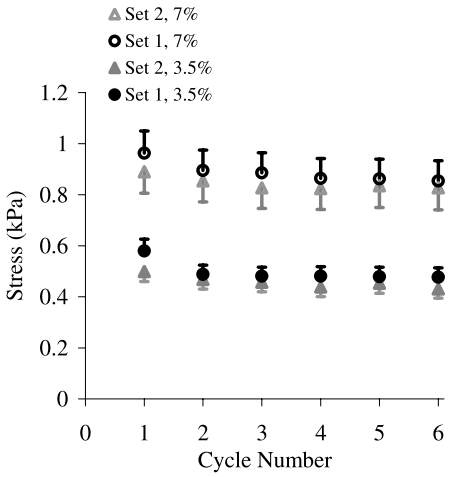

Fig. 5. Mean (±SE) stress per cycle measured at 3.5% and 7% ML extension. The data are for *Set 1* and *Set 2* averaged across the 5%, 10%, and 15% Stretches for 3.5% ML extension and 10% and 15% Stretches for 7% ML extension for all trabeculae ($n = 10$). There was no significant difference between *Set 1* and *Set 2*, demonstrating an absence of strain softening.

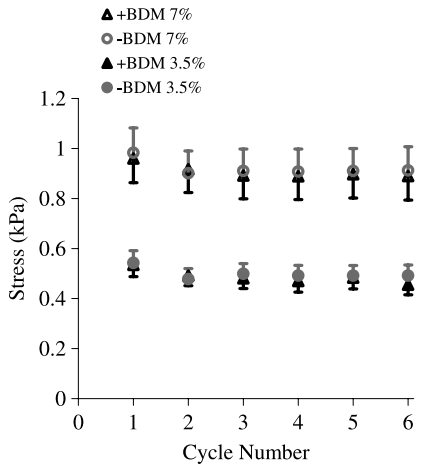

Fig. 7. Mean (±SE) stress per cycle (3.5% and 7% ML extensions) measured in +BDM and −BDM (for *Set 2* and *Set 3*). There was no statistically significant difference between stresses measured in +BDM and −BDM, implying that BDM does not alter the compliance of quiescent cardiac trabeculae.

Table 2. *ANOVA-derived P values of stresses at 3.5% and 7% ML for Sets 2 and Set 3*

	ML Extension	
	3.5%	7%
Order BDM presented	0.3433	0.3905
+BDM versus −BDM	0.4313	0.2822
Magnitude of Stretch (5%, 10%, and 15%)	0.3767	0.6998
Cycle (*1–6*)	0.0077	0.0012

Values shown are ANOVA-derived probabilities (*P* values) arising from tests of significance comparing stresses at 3.5% and 7% ML extension for *Set 2* and *Set 3*; $n = 9$ preparations. Note the lack of effect of BDM on compliance of quiescent trabeculae.

to materials that exhibit permanently increased compliance after the applied load, or stress, reaches a new maximum. Strain softening has been observed in intact cardiac tissue during both shear experiments on blocks of pig ventricular myocardium (12) and pressure inflation of whole rat hearts (13, 14). In both cases, strain softening was reported to be irreversible at physiologically relevant strains.

We found no evidence that strain softening occurs in intact rat cardiac trabeculae at physiologically relevant SL extensions (Table 1 and Figs. 2–4). Whereas a small viscoelastic stress relaxation effect was observed, this recovered fully between Sets (Fig. 3) as well as during the 30-s resting interval between Stretches (Fig. 2). We interpret this behavior as evidence of viscoelastic, reversible stress relaxation akin to the mechanical fatigue seen in single molecules of titin (25).

Possible causes of the previously reported strain softening at physiological strains include *1*) BDM, *2*) tissue microstructure, *3*) mode of deformation, *4*) fluid movement, *5*) ischemic anoxia and nonviability, *6*) cutting damage, or *7*) strain rate. These are considered in turn below.

BDM. In the studies performed by Emery et al. (13, 14) and Dokos et al. (12), the tissues were perfused with high concentrations of BDM (30 mM, 30 and 50 mM, respectively) before mechanical testing began. This was to protect the cardiac tissue from cutting injury (34) and to inhibit active contractile processes (38). Both Emery et al. and Dokos et al. speculated that the use of BDM might have contributed to the observed strain softening behavior, because BDM is known to increase the proportion of cross bridges in the weakly bound state. Our experiments showed no influence of BDM on strain softening or passive compliance in viable trabeculae (Table 1 and Fig. 7). Hence, we discount any contributions from BDM to the strain softening that has been observed by others.

Tissue microstructure. Strain softening in response to applied loads that are larger than normally observed in vivo is due to either plastic deformation or damage of collagen and other extracellular structures. In trabeculae, wavy perimysial collagen fibers are shown to straighten progressively when extended from a resting SL of 1.85 to 2.3 μm (20). Extension of cardiac tissue beyond a SL of 2.3 μm may well damage perimysial collagen and other extracellular matrix components to which the perimysial fibers are tethered. If the extracellular matrix is removed, cardiac titin exhibits strain softening above a SL of 3 μm (17, 27–29). Because extending sarcomeres beyond a length of 2.3 μm is reported to affect trabeculae viability (8), we kept the SL below 2.3 μm to avoid overextension of myocytes and the extracellular matrix.

Because trabeculae consist of an axial alignment of cardiac myocytes, our results imply that strain softening is absent during physiological extensions of intact viable myocytes. Likewise, Granzier and Irving (17) performed axial extensions of skinned cardiac myocytes from the rat and found no evidence of strain softening between SLs of 1.85 and 2.4 μm. Upon axial extension, isolated rabbit (29) and rat (27) myofibrils have demonstrated strain softening, but only when the SL was extended above 3 μm. Because the skinning process removed the entire extracellular matrix and collagen, Linke et al. (28) attributed the resulting development of passive force and strain softening at large extension to titin.

When single titin molecules from the rat were subjected to repeated stretch-and-release protocols, a rightward shift in the lower force region of the length-stress curve was observed (25). This mechanical fatigue recovered after a 4-min rest and thus was not strain softening, which, by definition, is an irreversible process. Similar softening behaviors have been observed in skinned rat myocytes from which actin filaments were removed (21) and where rest periods as short as 10 s allowed the passive stress to recover. This stress relaxation of the skinned myocytes was once again attributed to mechanical fatigue of titin because the extracellular matrix and actin filaments had been removed. From the results of these studies, we preclude titin as a source of irreversible strain softening.

There are microstructural differences between ventricular tissue and cardiac trabeculae. Ventricular tissue has a complex three-dimensional microstructural architecture that varies with location and depth across the ventricular wall (6, 26, 35, 44). Although trabeculae are often treated as homologous to ventricular tissue (20, 23), they have a simpler microstructure, consisting of axially aligned myocytes and large parallel perimysial collagen fibers (20). More complex microstructures may show strain softening behavior.

Mode of deformation. The mode of deformation applied in the present study was certainly different to those in previous reports of shear deformation of ventricular blocks (12) or volume inflation of whole hearts (13, 14). It is possible that shear or torsion experiments in trabeculae could exhibit strain softening.

Fluid movement. In both whole hearts and tissue blocks, strain softening could be partly due to extrusion of fluid from the vasculature and tissue. However, fluid shifts do not explain strain softening in the shear tests of Dokos et al. (12) because positive shear strain softening did not soften the negative shear stress-strain relationship.

Ischemic anoxia and nonviability. All experiments that have studied strain softening have employed nonperfused tissues. In our case, however, we are confident that the superfused trabeculae were not hypoxic, because they were smaller than the critical diameter (300 μm) at which an anoxic core arises in quiescent preparations (7). Furthermore, trabecula viability, assessed as the twitch force response to electrical stimulation, was confirmed between Sets. In contrast, in both the Emery et al. (13, 14) and Dokos et al. (12) studies, hearts were briefly perfused with high-potassium salt solutions containing BDM designed to induce arrest; thereafter, tissues were neither perfused nor superfused. The resulting ischemia may have induced changes in passive tissue properties and allowed rigor cross bridges to form.

Although BDM has been reported to delay the onset of rigor (1, 19, 22) and to reduce final rigor force in both metabolically challenged cardiac tissue (40) and skinned skeletal muscle (15), it does not prevent rigor bridge formation (1, 19, 22). Strain softening at low strain levels could, therefore, be a by-product of ischemia. If the ischemic period has allowed rigor cross bridges to form, then even a small SL extension may damage tissue, resulting in strain softening. In the present study, only preparations that remained viable (i.e., responsive to electrical stimulation) were included in the data analysis. It was noted that trabecula that were electrically nonresponsive (Fig. 6) showed classic strain softening behavior, together with elevated stress levels, compared with results from viable trabeculae (Fig. 2).

Cutting damage. In the present study, we confined cutting damage to blocks of tissue located well beyond the regions of stress measurement. As Dokos et al. (12) studied the shear behavior of blocks dissected from the ventricular wall, cutting damage was unavoidable, although possibly ameliorated by the presence of BDM (34). Studies that used isolated whole hearts avoided this problem entirely.

Strain rate. The ML extension velocity used in present study was 25 μm/s, which induced an approximate strain rate of 1% ML/s. Whereas this strain rate is lower than that observed during normal physiological operation, it is slightly larger than those used in studies that have demonstrated strain softening. A strain rate of 0.7% initial length (L_0)/s was applied during shear deformation of blocks of pig myocardium (12), whereas a strain rate of 0.3% was induced during inflation studies of rat hearts (13, 14). Because we used a strain rate higher than was used in any of these studies, the absence of strain softening cannot be attributed to our use of a low strain rate.

Effect of BDM on Passive Compliance

In the present study, there were no significant differences in trabeculae compliance in the presence or absence of BDM (Fig. 7). This lack of effect of BDM on compliance is consistent with the notion that there are relatively few force-bearing cross bridges in quiescent tissue. Similarly, BDM does not affect the passive force (29) or stiffness (28) generated by titin during a low extension stretch.

There is controversy in the literature concerning the presence of both weakly and strongly bound cross bridges in both the diastolic and quiescent states. The existence of weakly bound cross bridges has been investigated by measurement of instantaneous stiffness. With the use of this technique, studies have inferred both their presence (18, 36) and their absence (3, 8, 28). Similar controversy exists concerning the presence of strongly bound cross bridges during diastole. Studies using a variety of interventions, specimens, and indexes, in the absence of BDM, have provided evidence both for (31) and against (8, 24, 41) the existence of strongly bound, or force-bearing, cross bridges. Curiously, studies performed in the presence of BDM have shown comparably contradictory results (2, 19, 31, 39). Our results (Fig. 7 and Table 2) show a lack of effect of BDM on the compliance of intact rat cardiac trabeculae, thereby concurring with those studies that show a lack of measurable cross-bridge activity in quiescent tissue. This result, however, does not preclude the existence of cross-bridge activity during diastole, as such activity may cease during the long quiescent periods adopted during this study.

BDM has also been shown to increase diastolic pressure in isolated perfused whole hearts (32). A BDM-induced increase of slope of the end-diastolic pressure versus end-diastolic length relation (i.e., stiffness) has been reported in intact pig hearts (31). This was attributed to an increased tissue stiffness, or turgor ("garden hose effect"), which may have resulted from a BDM-induced dilation of the coronary vascular network. No corresponding increase of tension or stiffness is seen in papillary or trabecula preparations (Ref. 19 and present study), nor would any be expected due to this cause, because neither preparation was perfused.

Limitations

One reason for the lack of observable strain softening in the present study could have been accidental preconditioning of trabeculae during dissection or mounting. The utmost care was taken to avoid stretching the trabeculae during the dissection and mounting process, and the method of transferring the muscle from the dissection bath to the muscle bath via glass tubing was specifically designed to avoid the possibility of stretching. It is also possible that specimens could have moved or settled in the mounting hooks during Stretches. However, this would have been apparent by a sudden softening in the stress-strain relationship. As Fig. 6 demonstrates, strain softening was readily measurable by our apparatus in preparations that had stopped responding to electrical stimulation.

In conclusion, the present study has shown an absence of irreversible strain softening in viable, intact, rat cardiac trabeculae subjected to axial extensions within the physiological range regardless of the presence or absence of BDM. This absence of strain softening, in contrast to previously reported findings in other preparations (12–14), may be due to differences in tissue health, fluid movement, tissue microstructure, or the method of strain induction. The present study also found no effect of BDM on passive compliance, at least at the very low strain rates applied, consistent with studies on skinned cardiac myocytes, myofibrils, and titin molecules.

GRANTS

We acknowledge the generous financial support of the Royal Society of New Zealand (Marsden Fund) and the Health Research Council of New Zealand.

REFERENCES

1. **Armstrong SC and Ganote CE.** Effects of 2,3-butanedione monoxime (BDM) on contracture and injury of isolated rat myocytes following metabolic inhibition and ischemia. *J Mol Cell Cardiol* 23: 1001–1014, 1991.
2. **Backx PH, Gao WD, Azan-Backx MD, and Marban E.** Mechanism of force inhibition by 2,3-butanedione monoxime in rat cardiac muscle: roles of $[Ca^{2+}]_i$ and cross-bridge kinetics. *J Physiol* 476: 487–500, 1994.
3. **Bagni MA, Cecchi G, Colomo F, and Garzella P.** Are weakly binding bridges present in resting intact muscle fibers? *Biophys J* 63: 1412–1415, 1992.
4. **Brady AJ.** Length-tension relations in cardiac muscle. *Am Zool* 7: 603–611, 1967.
5. **Brady AJ.** Mechanical properties of isolated cardiac myocytes. *Physiol Rev* 71: 413–427, 1991.
6. **Caulfield JB and Borg TK.** The collagen network of the heart. *Lab Invest* 40: 364–372, 1979.
7. **Daut J and Elzinga G.** Heat production of quiescent ventricular trabeculae isolated from guinea-pig heart. *J Physiol* 398: 259–275, 1988.

8. **De Tombe PP and ter Keurs HE.** An internal viscous element limits unloaded velocity of sarcomere shortening in rat myocardium. *J Physiol* 454: 619–642, 1992.
9. **De Tombe PP and ter Keurs HEDJ.** Force and velocity of sarcomere shortening in trabeculae from rat heart. *Circ Res* 66: 1239–1254, 1990.
10. **Demer LL and Yin FC.** Passive biaxial mechanical properties of isolated canine myocardium. *J Physiol* 339: 615–630, 1983.
11. **Dobesh DP, Konhilas JP, and de Tombe PP.** Cooperative activation in cardiac muscle: impact of sarcomere length. *Am J Physiol Heart Circ Physiol* 282: H1055–H1062, 2002.
12. **Dokos S, Smaill BH, Young AA, and LeGrice IJ.** Shear properties of passive ventricular myocardium. *Am J Physiol Heart Circ Physiol* 283: H2650–H2659, 2002.
13. **Emery JL, Omens JH, Mathieu-Costello OA, and McCulloch AD.** Structural mechanisms of acute ventricular strain softening. *Int J Cardiol* 1: 241–250, 1998.
14. **Emery JL, Omens JH, and McCulloch AD.** Strain softening in rat left ventricular myocardium. *J Biomech Eng* 119: 6–12, 1997.
15. **Fryer MW, Neering IR, and Stephenson DG.** Effects of 2,3-butanedione monoxime on the contractile activation properties of fast- and slow-twitch rat muscle fibres. *J Physiol* 407: 53–75, 1988.
16. **Fung YC.** *Biomechanics: Mechanical Properties of Living Tissues*. New York: Springer-Verlag, 1993, p. 437.
17. **Granzier HL and Irving TC.** Passive tension in cardiac muscle: contribution of collagen, titin, microtubules, and intermediate filaments. *Biophys J* 68: 1027–1044, 1995.
18. **Granzier HL and Wang K.** Passive tension and stiffness of vertebrate skeletal and insect flight muscles: the contribution of weak cross-bridges and elastic filaments. *Biophys J* 65: 2141–2159, 1993.
19. **Hajjar RJ, Ingwall JS, and Gwathmey JK.** Mechanism of action of 2,3-butanedione monoxime on contracture during metabolic inhibition. *Am J Physiol Heart Circ Physiol* 267: H100–H108, 1994.
20. **Hanley PJ, Young AA, LeGrice IJ, Edgar SG, and Loiselle DS.** 3-Dimensional configuration of perimysial collagen fibres in rat cardiac muscle at resting and extended sarcomere lengths. *J Physiol* 517: 831–837, 1999.
21. **Helmes M, Trombitas K, Centner T, Kellermayer M, Labeit S, Linke WA, and Granzier H.** Mechanically driven contour-length adjustment in rat cardiac titin's unique N2B sequence: titin is an adjustable spring. *Circ Res* 84: 1339–1352, 1999.
22. **Ikenouchi H, Zhao L, and Barry WH.** Effect of 2,3-butanedione monoxime on myocyte resting force during prolonged metabolic inhibition. *Am J Physiol Heart Circ Physiol* 267: H419–H430, 1994.
23. **Johnson EA and Sommer JR.** A strand of cardiac muscle. Its ultrastructure and the electrophysiological implications of its geometry. *J Cell Biol* 33: 103–129, 1967.
24. **Kass DA, Wolff MR, Ting CT, Liu CP, Chang MS, Lawrence W, and Maughan WL.** Diastolic compliance of hypertrophied ventricle is not acutely altered by pharmacologic agents influencing active processes. *Ann Intern Med* 119: 466–473, 1993.
25. **Kellermayer MS, Smith SB, Bustamante C, and Granzier HL.** Mechanical fatigue in repetitively stretched single molecules of titin. *Biophys J* 80: 852–863, 2001.
26. **Le Grice IJ, Smaill BH, Chai LZ, Edgar SG, Gavin JB, and Hunter PJ.** Laminar structure of the heart: ventricular myocyte arrangement and connective tissue architecture in the dog. *Am J Physiol Heart Circ Physiol* 269: H571–H582, 1995.
27. **Linke WA, Bartoo ML, Ivemeyer M, and Pollack GH.** Limits of titin extension in single cardiac myofibrils. *J Muscle Res Cell Motil* 17: 425–438, 1996.
28. **Linke WA, Ivemeyer M, Labeit S, Hinssen H, Rueegg JC, and Gautel M.** Actin-titin interaction in cardiac myofibrils: probing a physiological role. *Biophys J* 73: 905–919, 1997.
29. **Linke WA, Popov VI, and Pollack GH.** Passive and active tension in single cardiac myofibrils. *Biophys J* 67: 782–792, 1994.
30. **Liu X and Pollack GH.** Mechanics of F-actin characterized with microfabricated cantilevers. *Biophys J* 83: 2705–2715, 2002.
31. **Lu L, Xu Y, Zhu P, Greyson C, and Schwartz GG.** A common mechanism for concurrent changes of diastolic muscle length and systolic function in intact hearts. *Am J Physiol Heart Circ Physiol* 280: H1513–H1518, 2001.
32. **Marijic J, Buljubasic N, Stowe DF, Turner LA, Kampine JP, and Bosnjak ZJ.** Opposing effects of diacetyl monoxime on contractility and calcium transients in isolated myocardium. *Am J Physiol Heart Circ Physiol* 260: H1153–H1159, 1991.
33. **Mirsky I and Rankin JS.** The effects of geometry, elasticity, and external pressures on the diastolic pressure-volume and stiffness-stress relations. How important is the pericardium? *Circ Res* 44: 601–611, 1979.
34. **Mulieri LA, Hasenfuss G, Ittleman F, Blanchard EM, and Alpert NR.** Protection of human left ventricular myocardium from cutting injury with 2,3-butanedione monoxime. *Circ Res* 65: 1441–1449, 1989.
35. **Nielsen PMF, Le Grice IJ, Smaill BH, and Hunter PJ.** Mathematical model of geometry and fibrous structure of the heart. *Am J Physiol Heart Circ Physiol* 260: H1365–H1378, 1991.
36. **Schoenberg M.** Characterization of the myosin adenosine triphosphate (M.ATP) crossbridge in rabbit and frog skeletal muscle fibers. *Biophys J* 54: 135–148, 1988.
37. **Schouten VJA and ter Keurs HEDJ.** The force-frequency relationship in rat myocardium: the influence of muscle dimensions. *Pflügers Arch* 407: 14–17, 1986.
38. **Sellin LC and McArdle JJ.** Multiple effects of 2,3-butanedione monoxime. *Pharmacol Toxicol* 74: 305–313, 1994.
39. **Sollott SJ, Ziman BD, Warshaw DM, Spurgeon HA, and Lakatta EG.** Actomyosin interaction modulates resting length of unstimulated cardiac ventricular cells. *Am J Physiol Heart Circ Physiol* 271: H896–H905, 1996.
40. **Stapleton MT, Fuchsbauer CM, and Allshire AP.** BDM drives protein dephosphorylation and inhibits adenine nucleotide exchange in cardiomyocytes. *Am J Physiol Heart Circ Physiol* 275: H1260–H1266, 1998.
41. **Stuyvers BD, Miura M, Jin JP, and ter Keurs HE.** Ca^{2+}-dependence of diastolic properties of cardiac sarcomeres: involvement of titin. *Prog Biophys Mol Biol* 69: 425–443, 1998.
42. **Ter Keurs HE, Rijnsburger WH, van Heuningen R, and Nagelsmit MJ.** Tension development and sarcomere length in rat cardiac trabeculae. Evidence of length-dependent activation. *Circ Res* 46: 703–714, 1980.
43. **Wiggins JR, Reiser J, Fitzpatrick DF, and Bergey JL.** Inotropic actions of diacetyl monoxime in cat ventricular muscle. *J Pharmacol Exp Ther* 212: 217–212, 1980.
44. **Young AA, Legrice IJ, Young MA, and Smaill BH.** Extended confocal microscopy of myocardial laminae and collagen network. *J Microsc* 192: 139–150, 1998.
45. **Zhao Y and Kawai M.** Kinetic and thermodynamic studies of the cross-bridge cycle in rabbit psoas muscle fibers. *Biophys J* 67: 1655–1668, 1994.